Viscosity of a one-component polarizable fluid

J. M. Sun and R. Tao
Department of Physics, Southern Illinois University, Carbondale, Illinois 62901
(Received 17 January 1995)

The viscosity of a one-component polarizable fluid in an electric field is studied by computer simulations. The fluid viscosity increases with the field through three stages. In a weak field, the fluid remains Newtonian, although its viscosity increases. At this stage, while drifting in the flow direction, particles diffuse in the direction perpendicular to the flow. In an intermediate electric field, the fluid has tilted and broken chains moving with the flow and the fluid becomes non-Newtonian. The viscosity η and the shear rate $\dot{\gamma}$ have the relationship $\eta=\eta_0 e^{-\dot{\gamma}\tau}$, where τ is the relaxation time and η_0 is exponentially proportional to the dipolar interaction energy and the volume fraction. In a strong electric field, the fluid contains condensed chains that provide yield stress and hysteresis.

PACS number(s): 82.70.Gg, 61.90.+d, 64.90.+b

I. INTRODUCTION

One-component polarizable fluids are interesting physics systems which have important applications. We can define these fluids as aggregates of particles which can be strongly polarized in an external electric field. If the particles have a permanent dipole moment, the polarization can be a result of alignment of the dipoles in the field direction. If the particles have no permanent dipole moment, the polarization can be induced by the electric field because of the dielectric-constant or conductivity mismatch between the particles and the medium.

The early work of Andrade and Dodd showed that one-component polarizable liquids placed in a strong electric field would have a significant increase of viscosity while nearly no effect was seen on the viscosity of nonpolar liquids [1]. A recent discovery of the electrorheological (ER) effect of liquid crystal polymer solution greatly enhances the interest of research in this area [2].

A conventional ER fluid is made of fine dielectric particles suspended in a liquid of low dielectric constant [3–7]. The large contrast of dielectric constant between the particles and the liquid makes the system easily polarizable in an electric field. The electric-field induced change of viscosity in ER fluids has provided opportunities for many new technological applications [3]. The crucial point of ER application is now in materials technology. Because of the density mismatch between the particles and the liquid, settling is a problem in some conventional ER fluids. Some applications, such as ER clutch, require ER fluids with a much stronger yield stress. The strong ER effect of liquid crystal polymer solutions has broadened our horizon in search for good ER fluids. Especially, since one-component polarizable liquids have no problem in settling, they may be suitable for applications which cannot tolerate any settling.

In this paper, we will investigate the viscosity of one-component polarizable liquid in Couette geometry via computer simulations. Our model and the details of simulations are presented in Sec. II. In Sec. III, we discuss our results. Our findings indicate that the viscosity of one-component polarizable fluid increases with an electric field through three stages. In a weak field, the fluid remains Newtonian although its viscosity increases with the field. At this stage, while drifting in the flow direction, particles diffuse in the direction perpendicular to the flow. In an intermediate electric field, the fluid has tilted and broken chains moving with the flow and the fluid becomes non-Newtonian. The viscosity η and the shear rate $\dot{\gamma}$ has the following relationship $\eta=\eta_0 e^{-\dot{\gamma}\tau}$, where τ is a relaxation time and η_0 is exponentially proportional to the dipolar energy and the volume fraction. In a strong electric field, the fluid contains condensed chains which produce a yield stress and hysteresis.

II. MODEL AND SIMULATIONS

Our three-dimensional system is based on the dipole model frequently used in the study of ER fluids [8]. This model is reasonably good when the particle concentration is low, although it has limitation when the concentration is high. We have N particles placed between two parallel electrodes which are planes $z=L/2$ and $z=-L/2$ (see Fig. 1). The motion of each particle is determined by a classical motion equation. The electric force on each particle is the sum of dipolar forces exerted by other particles as well as by images. Experiments have shown that an electric field parallel to the flow direction has little effect on the liquid viscosity. Therefore, we examine the case in which the flow is moving along the x direction while the applied electric field is along the z direction. In both x and y directions, a periodic boundary condition is imposed. Thus, a particle in Fig. 1 moving out of the box returns to the box from the opposite side with the same velocity.

We introduce two wall layers which are adjacent to each electrode, respectively. The particles in the wall layers are distinct from the particles in the flow (bulk particles). While the bulk particles are allowed to move in all

 ©1995 The American Physical Society

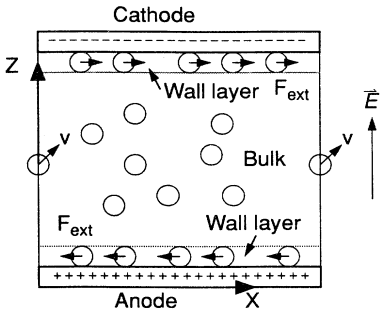

FIG. 1. A sketch of our model.

three directions, the wall-layer particles are only allowed to move in the x and y directions and are not allowed to exchange with the bulk particles. Thus, the wall particles cannot leave the electrode they attach. In addition to the dipolar interactions, the wall particles adjacent to the top electrode experience an external force in the x direction and the wall particles adjacent to the bottom electrode experience an external force in the opposite x direction. As these shear forces act on the wall particles, a velocity gradient in the z direction is established.

Our wall layers are based on observations made in ER fluid flow experiments which find two layers of dielectric particles cumulated on the two electrodes, distinct from the particles in the flow. Ashurst and Hoover also used similar wall layers in their simulation of dense fluid shear flow [9].

In an electric field, each particle obtains an induced dipole moment, $\vec{p}=\alpha\epsilon_f(\sigma/2)^3\vec{E}_{\rm loc}$ where $\alpha=(\epsilon_p-\epsilon_f)/(\epsilon_p+2\epsilon_f)$ and $\vec{E}_{\rm loc}$ is the local field. The motion of the ith particle is described by a classical equation

$$md^2\vec{r}_i/dt^2=\vec{F}_i \ , \tag{2.1}$$

where $\vec{F}_i$ is the total force acting on it.

The dipolar force acting on the particle at $\vec{r}_i$ by a particle at $\vec{r}_j$ is given by

$$\vec{f}_{ij}=\frac{3p^2}{\epsilon_f r_{ij}^4}[\vec{e}_r(1-3\cos^2\theta_{ij})-\vec{e}_\theta\sin(2\theta_{ij})] \ , \tag{2.2}$$

where $\vec{r}_{ij}=\vec{r}_i-\vec{r}_j$ and $0\le\theta_{ij}\le\pi/2$ is the angle between the z direction and the joint line of the two dipoles. We use $\vec{e}_r$ as a unit vector parallel to $\vec{r}_{ij}$ and $\vec{e}_\theta$ as a unit vector parallel to $\vec{e}_r\times(\vec{e}_r\times\vec{E}_0)$.

A dipole $\vec{p}$ inside the capacitor at $\vec{r}_i=(x_i,y_i,z_i)$ produces an infinite number of images at $(x_i,y_i,-z_i)$ and $(x_i,y_i,2Lk\pm z_i)$ for $k=\pm1,\pm2,\ldots$. The force between a dipole and an image has the same form as Eq. (2.2). The jth particle and its infinite images produce an electric force on the ith particle [8,10],

$$\begin{aligned}
f_{ij,x}&=\frac{p^2}{\epsilon_f L^4}\sum_{s=1}^{\infty}\frac{4s^2\pi^3(x_i-x_j)}{\rho_{ij}}K_1\left[\frac{s\pi\rho_{ij}}{L}\right]\\
&\quad\times\cos\left[\frac{s\pi z_i}{L}\right]\cos\left[\frac{s\pi z_j}{L}\right] \ ,\\
f_{ij,y}&=\frac{p^2}{\epsilon_f L^4}\sum_{s=1}^{\infty}\frac{4s^3\pi^3(y_i-y_j)}{\rho_{ij}}K_1\left[\frac{s\pi\rho_{ij}}{L}\right]\\
&\quad\times\cos\left[\frac{s\pi z_i}{L}\right]\cos\left[\frac{s\pi z_j}{L}\right] \ ,\\
f_{ij,z}&=\frac{p^2}{\epsilon_f L^4}\sum_{s=1}^{\infty}4s^3\pi^3K_0\left[\frac{s\pi\rho_{ij}}{L}\right]\sin\left[\frac{s\pi z_i}{L}\right]\\
&\quad\times\cos\left[\frac{s\pi z_j}{L}\right] \ ,
\end{aligned} \tag{2.3}$$

where $\rho_{ij}=\sqrt{(x_i-x_j)^2+(y_i-y_j)^2}$ and K_0 and K_1 are modified Bessel functions. The force on the ith particle by its own images is in the z direction and denoted as $\vec{f}_i^{\rm self}$,

$$f_{i,z}^{\rm self}=\frac{3p^2}{8\epsilon_f}\left[-\frac{1}{z_i^4}+\sum_{s=1}^{\infty}\left[\frac{1}{(z_i-sL)^4}-\frac{1}{(z_i+sL)^4}\right]\right] . \tag{2.4}$$

In addition to the dipolar interactions, two spheres repel each other strongly whenever they are colliding with each other. This short-range repulsive force is important in preventing particles from collapsing. There have been several forms of this short-range interaction in the study of ER fluids, ranging from a hard-core interaction, soft-core, to a power rule [8,11]. In our model, we follow Melrose [12] to use a power rule,

$$\vec{f}_{ij}^{\rm rep}\sim\vec{r}_{ij}/r_{ij}^{n+2} \ , \tag{2.5}$$

where $\vec{r}_{ij}=\vec{r}_i-\vec{r}_j$. It is clear that as n increases, the short-range force becomes stronger. The results reported here are related to $n=23$, a value large enough to prevent the particles from collapsing. We have checked the situation of a different n and found that although the value of n affects the initial motion of the particles because of collisions, it has little effect on the final value of viscosity which is measured after a dynamic equilibrium is established.

When a particle in the flow collides with an electrode, we take the collision as a complete elastic collision which maintains the particle's speed but reverses the sign of the z component of the velocity. This arrangement prevents any particle in the flow from moving out of the electrodes.

Now for the bulk particles $\vec{F}_i$ in Eq. (2.1) is given by

$$\vec{F}_i=\sum_{j\neq i}(\vec{f}_{ij}+\vec{f}_{ij}^{\rm rep})+\vec{f}_i^{\rm self} \ . \tag{2.6}$$

As mentioned earlier, the wall particles are experiencing additional external forces in the x direction which produce the shear flow.

A viscous flow always produces heat which may cause

temperature increase if the heat is not removed. In our simulations, the temperature in a layer is defined by the following equation:

$$T=\frac{m}{2k_B(N_l-1)}\sum_{i=1}^{N_l}(\vec{v}_i-\vec{v}_a)^2 , \tag{2.7}$$

where N_l is the number of particles in the layer and the average velocity $\vec{v}_a$ is given by

$$\vec{v}_a=\sum_{i=1}^{N_l}\vec{v}_i/N_l . \tag{2.8}$$

In Eq. (2.7) the denominator has N_l-1 rather than N_l because the center of mass is also moving. To maintain the temperature at a constant T_0, we apply a renormalization procedure to the wall layers and the two layers immediately adjacent to the wall layers.

$$\vec{v}_i^R=\vec{v}_a+(\vec{v}_i-\vec{v}_a)\sqrt{T_0/T} , \tag{2.9}$$

where T is determined by Eq. (2.7) and $\vec{v}_a$ is given in Eq. (2.8). This is equivalent to removing heat in the system from the two electrodes.

In our simulations, the electrodes have $L_x=L_y=16a$ while the distance between the electrodes is $L=14a$. We denote a as the particle radius. Each wall layer has 20 particles. There are another 100 particles in the bulk. The volume fraction is thus 16.4% which is quite low and makes the dipole model valid. Our theoretical calculation has already shown that when $L_z\leq 12a$, a single-chain structure is the preferred solid structure in ER fluids; only when $L_z>12a$, ER fluids are able to have thick columns [13]. In real experiments, a has the order of micrometer, while L_z has the order of millimeter. Therefore, we take $L_z=14a$ to satisfy the above condition.

Initially, the particles are distributed randomly into the space with a velocities distribution corresponding to T_0. The applied forces on the wall-layer particles drive them to flow. The parameter λ measures the dipolar energy to the thermal energy and also indicates the strength of the electric field [14],

$$\lambda=p^2/(a^3k_BT_0) . \tag{2.10}$$

In our simulations, we use $\sqrt{mk_BT/a^4}$ as the unit of viscosity, $\sqrt{ma^2/k_BT}$ as the unit of time, and $\sqrt{k_BT/ma^2}$ as the unit of shear rate.

We have applied a fourth-order Runge-Kutta method of a fixed step size to integrate Eq. (2.1). The step size is $0.02\sqrt{ma^2/(k_BT_0)}$. If $T_0=300$ K, $a=1.0$ μm, and the particles have density $\rho=1.2$ g/cm^3, then one step is about 2×10^{-5} s.

For one value of λ, we vary the shear stress to obtain the effective viscosity as a function of $\dot{\gamma}$ and λ. The variation of shear stress is as smooth as possible. After the shear stress changes, we run the system at least 20 000 steps to establish a dynamic equilibrium state. For the above example, 20 000 steps correspond to 0.4 s. In the dynamic equilibrium state, we measure the velocity distribution and determine the shear rate $\dot{\gamma}$. In most cases, we find a laminate flow. If the total force acting on one wall layer is F, then the shear stress $S=F/(L_xL_y)$. The effective viscosity is determined by

$$\eta=S/\dot{\gamma} . \tag{2.11}$$

TABLE I. Shear flow at $\lambda=55$ and $\dot{\gamma}=0.0947\sqrt{k_BT/ma^2}$.

Layer	Average no. of particles	Average v_x	Temperature
1	19.3	−0.383	1.000
2	19.2	−0.172	1.048
3	19.2	0.023	1.057
4	19.2	0.199	1.047
5	19.5	0.379	1.000

III. RESULTS AND DISCUSSIONS

A typical velocity profile and average temperature in each flow layer is listed in Table I. As mentioned in Sec. II, at each step, we extricate heat from the two wall layers and the two layers immediately adjacent to the wall layers. Table I shows that this approach works well in keeping the bulk nearly uniform in temperature although the middle layer still has a slightly higher temperature. This situation is normal because we assume that the heat dissipates from the two electrodes. In Fig. 2, we plot the velocity distribution. It is clear that the system has a laminate flow and the slope of the velocity line is related to the shear rate. When the external shear force is small, the velocity distribution may deviate from a straight line. The example in Fig. 3 shows that the middle layers have a lower shear rate than the layers close to the electrodes. It is also understandable that there are more fluctuations when the average shear rate is low.

A. Newtonian flow

At a low λ, i.e., a weak field, our simulations find a good Newtonian flow. In Fig. 4, we plot the effective viscosity as a function of shear rate at $\lambda=10$ and 35. As shown there, the effective viscosity is independent on the shear rate. The parallel line is a clear indication of a

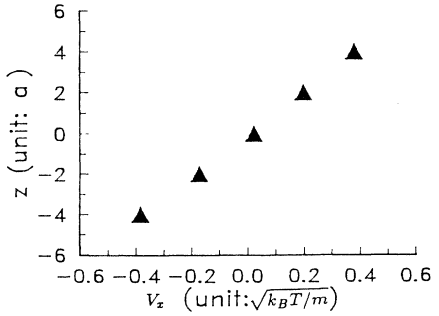

FIG. 2. Velocity profile of a laminate flow at $\lambda=35$ and $\dot{\gamma}=0.095\sqrt{k_BT/ma^2}$.

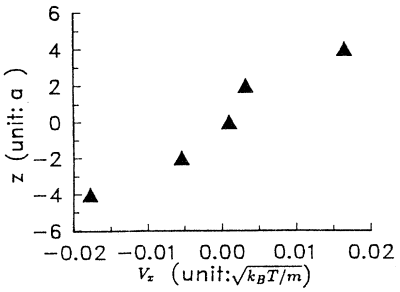

FIG. 3. Velocity profile at $\lambda=90$ and $\dot{\gamma}=0.004\sqrt{k_BT/ma^2}$. When the external shear force is small, the middle layers have a lower shear rate than the layers close to the electrodes.

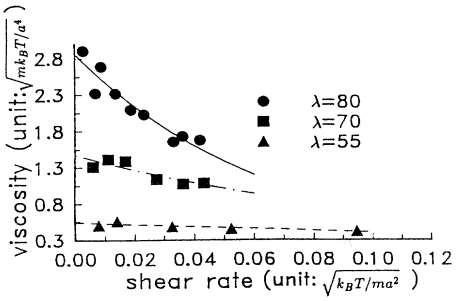

FIG. 5. Viscosity versus shear rate at large λ ($\lambda=55$, 70, and 80).

Newtonian fluid. The result is similar to a neutral dilute fluid. In our simulations, we also have a low volume fraction 16.4%.

B. Non-Newtonian flow

At a high field, the flow shows non-Newtonian characteristics. In Fig. 5, we plot the viscosity as a function of the shear rate $\dot{\gamma}$ for $\lambda=55$, 70, and 80. The effective viscosity is increasing as the shear rate is reducing. The changes in the rheological behaviors can be interpreted as a transition from the streaming type of transport to a potential type of transport where the interchanges of momentum between layers are mainly accomplished through potential interaction.

For a fluid with a strong intermolecular interaction, the dependence of viscosity on shear rate can be described by the Ree-Eyring relation [15], $\eta=(\eta_0/\tau\dot{\gamma})\sinh^{-1}(\tau\dot{\gamma})$ where η_0 is the viscosity at zero shear rate and τ is the relaxation time of the system.

In ER fluids, a power rule $\eta\sim\dot{\gamma}^{-\Delta}$ has been suggested [16]. This suggestion is based on a rotation of induced ER solid structure in a shear flow. Therefore, in order to have the power rule, the ER fluid must have nonzero yield stress.

However, our system at $\lambda=55-80$ still has zero shear stress for $\dot{\gamma}=0$; therefore, it is still a liquid and the power rule does not apply. The viscosity is plotted in Fig. 5. From the curve, we have found that the viscosity fits the following relationship:

$$\eta=\eta_0 e^{-\dot{\gamma}\tau}\ , \tag{3.1}$$

where τ can be also defined as a relaxation time. For $\lambda=55$, 70, and 80 we have $\tau=3.0$, 7.55, and 14.53 (unit: $\sqrt{ma^2/k_BT}$). The relaxation time increases with the increasing of the electric field. This is consistent with the fact that the stronger the electric field is, the longer is the time for the system to reach its dynamic equilibrium state.

The Eyring theory has viscosity of a normal liquid expressed as [17]

$$\eta=A\exp(\Delta E/k_BT)\ , \tag{3.2}$$

where ΔE is the energy barrier required to open up a hole for the transposed particle to move from one potential minimum to another minimum. Similar to the Eyring theory, in our polarized liquid, ΔE should also be related to an energy barrier to open a hole to let a particle move from one potential minimum to another one. The leading term of this energy barrier has the order of the dipolar energy p^2/a^3. In addition, it is easy to open a hole when the volume fraction ϕ is low and vice versa. Therefore, we expect the viscosity at zero shear rate, η_0, has the following form:

$$\eta_0=c_0\exp[b\phi p^2/(a^3k_BT)]\ , \tag{3.3}$$

where c_0 and b are constants. In Fig. 6, we plot η_0

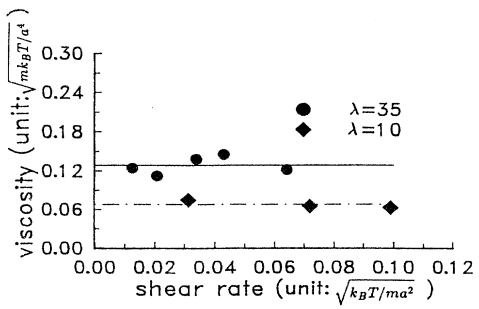

FIG.4 Viscosity versus shear rate at small λ ($\lambda=10$ and 35).

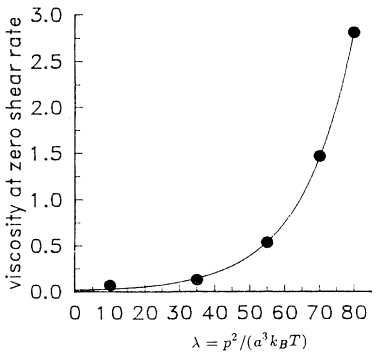

FIG. 6. Viscosity at zero shear rate versus λ. The solid line is the exponential fitting.

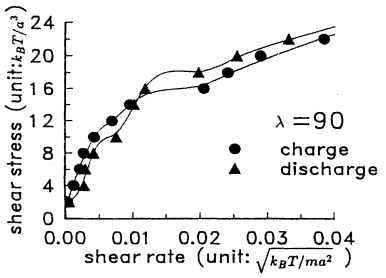

FIG. 7. Shear stress versus shear rate at $\lambda=90$. The discharge does not follow the same route of the charge curve, indicating a hysteresis.

against λ and find the curve fits the above relationship very well. The two fitting constants are $c_0=0.014$ and $b=0.402$. We want to emphasize that Eq. (3.3) is only valid for the liquid state. In deriving Eq. (3.3), we only consider the contribution of dipolar interactions. Therefore, when λ is small, Eq. (3.3) may underestimate the viscosity, because the other contributions to the viscosity cannot be ignored.

C. Bingham plastic

At $\lambda=90$, we observe a different phenomenon. There is a yield stress which has a value between $2k_BT/a^3$ to $4k_BT/a^3$. The particles do not move when the applied stress is below the yield stress. Only if the applied shear stress exceeds the yield stress, a flow is formed. Therefore, our system becomes a Bingham plastic. There is also clearly a hysteresis. The relationship between shear rate and shear stress depends on the flow history now. Similar hysteresis in experiments of ER fluids has been reported by Lemaire, Bossis, and Grasselli [18]. In our simulations, we first increase the shear stress at a rate $2k_BT/a^3$ in 100 000 time steps. Then we decrease the shear stress at the same rate. The simulation result is shown in Fig. 7. It is clear that the discharge does not follow the same route of the charge curve, indicating a hysteresis. The difference in the shear rate at a same shear stress can be as high as 60%. At this stage, the suggested power rule between the effective viscosity and the shear rate may apply [16]. However, for the simulations at this stage it becomes very difficult to produce repeatable results. A further investigation is needed.

D. Structural change

All these changes of rheology with the field can be related to the change of structure of the polarizable fluid under an electric field. Although the work reported here focuses on the effective viscosity, we have paid some attention to the movements of particles.

In Fig. 8, we plot a typical particle motion in the z direction at different electric fields. For a small electric field, such as $\lambda=35$, the particles wander up and down in the z direction while drifting along the x direction. This characterizes a diffusive motion which provides a momentum transfer between different layers. This motion behavior explains why the liquid is a Newtonian fluid. At a strong electric field, such as at $\lambda=90$, the particle has little motion in the z direction.

In Fig. 9, we plot an instant microscopic flow structure at $\lambda=35$. In order to have a clear view, we only show a slab of the flow, parallel to the x-z plane. It is clear there that the system has no obvious ordering; therefore, it is a Newtonian liquid.

At $\lambda=70$ the particles do not wander in the z direction, although we see some oscillations around its equilibrium position in the z direction. The instant microscopic flow structure is shown in Fig. 10. The flow has tilted chains and broken chains. These chains are distinct and well separated. The tilting is caused by the sheared motion. This indicates that the dipolar interactions play a much more important role than the diffusion now. Therefore, the fluid shows non-Newtonian behavior.

At $\lambda=90$ the particles are tightly bound to their equilibrium position in the z direction with very small fluctuations. The dominant contribution to the viscosity is the dipolar interactions. The microscopic flow structure shows chains condensed (Fig. 11). In fact, a number of chains are clinging to each other to form a thick and stable structure. This structure provides a yield stress to the system and hysteresis.

In concluding our paper, we should point out that our

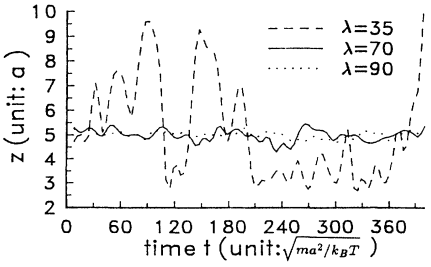

FIG. 8. A typical particle motion in the z direction at different electric fields. At a small electric field, the particles wander up and down in the z direction, but at a strong electric field, the particle moves little in the z direction.

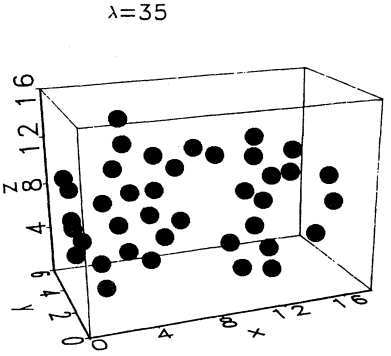

FIG. 9. An instant slab of flow at $\lambda=35$, parallel to the x-z plane. The system has no obvious ordering. Length unit is a.

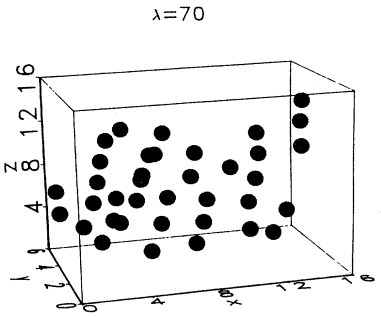

FIG. 10. An instant slab of flow at $\lambda=70$, parallel to the x-z plane. There are tilted chains and broken chains, well separated. Length unit is a.

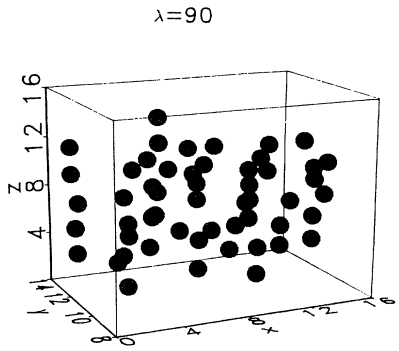

FIG. 11. An instant slab of flow at $\lambda=90$, parallel to the x-z plane. A number of chains are clinging to each other to form a thick and stable structure. Length unit is a.

simulations were performed on an IBM vectorized supercomputer; a system of 140 particles in the simulations is small in comparison to a real system. However, to tackle a much larger system on our present computer is almost formidable. In order to see the finite size effect, we have done some experiments. For example, we have conducted simulations under different L_x and L_y while L_xL_y, i.e., the volume fraction, remains unchanged. Since the viscosity of the new system has little change, the finite size effect seems to be insignificant. Therefore, we believe that our numerical results can provide some insight to experiments and be served as a base for future analytical work.

In addition, the volume fraction 16.4% in our simulations is low. If the volume fraction increases, the dipole model will be limited. However, we expect that the three stages in the viscosity change are still valid. However, it is conceivable that with the fluid at a higher volume fraction it will be easier to show non-Newtonian behavior and have a yield stress. The relationship between the flow structure and viscosity change should be further investigated.

ACKNOWLEDGMENTS

This research is supported by a grant from Illinois Consortium for Advanced Radiation Sources and by the Office of Naval Research Grant No. N00014-93-1-0582.

[1] E. N. Andrade and C. Dodd, Proc. R. Soc. London Ser. A **187**, 296 (1946); A **204**, 449 (1951).
[2] I. K. Yang and A. D. Shine, J. Rheol. **36**, 1079 (1992).
[3] W. M. Winslow, J. Appl. Phys. **20**, 1137 (1949).
[4] For example, see *Electrorheological Fluids,* edited by R. Tao, and G. D. Roy (World Scientific, Singapore, 1994).
[5] R. Tao, J. T. Woestman, and N. K. Jaggi, Appl. Phys. Lett. **55**, 1844 (1989).
[6] H. Block and J. P. Kelly, US Patent No. 4,687,589 (1987).
[7] F. E. Filisko and W. E. Armstrong, US Patent No. 4,744,914 (1988).
[8] R. Tao and Q. Jiang, Phys. Rev. Lett. **73**, 205 (1994).
[9] W.T. Ashurst and W. G. Hoover, Phys. Rev. A **11**, 658 (1975).
[10] R. Tao, Phys. Rev. E **47**, 423 (1993).
[11] D. J. Klingenberg, F. van Swol, and C. F. Zukoski, J. Chem. Phys. **91**, 7888 (1989).
[12] J. R. Melrose, Phys. Rev. A **44**, R4787 (1991).
[13] R. Tao and J. M. Sun, Phys. Rev. Lett. **67**, 398 (1991).
[14] P. M. Adriani and A. P. Gast, Phys. Fluids **31**, 2757 (1988).
[15] F. H. Ree, T. Ree, and H. Eyring, Ind. Eng. Chem. **50**, 136 (1958).
[16] T. C. Halsey, J. E. Martin, and D. Adolf, Phys. Rev. Lett **68**, 1519 (1992).
[17] H. Eyring, J. Chem. Phys. **4**, 283 (1936).
[18] E. Lamaire, G. Bossis, and Y. Grasselli, Langmuir **8**, 2957 (1992).